Carbohydrate Polymers 106 (2014) 432–439

Contents lists available at ScienceDirect

Carbohydrate Polymers

journal homepage: www.elsevier.com/locate/carbpol

Starch-based nanocomposites: A comparative performance study of cellulose whiskers and starch nanoparticles

Rasool Nasseri, Naser Mohammadi*

Department of Polymer Engineering and Color Technology, Amirkabir University of Technology, P.O. Box 15875-4413, 424 Hafez Avenue, Tehran, Iran

ARTICLE INFO

Article history:
Received 19 July 2013
Received in revised form 7 January 2014
Accepted 9 January 2014
Available online 19 January 2014

Keywords:
Plasticized starch
Reinforcement
Cellulose whiskers
Starch nanoparticles
Surface phenomenon
Transcrystallization

ABSTRACT

A comparative performance study of cellulose whiskers (CW) and starch nanoparticles (SN) on plasticized starch (PS) reinforcement has been presented. In order to study the involved surface phenomena, CW and SN were extracted through acid hydrolysis using sulfuric acid to fulfill the similar surface groups and interactions. CW-filled and SN-filled nanocomposites were then prepared with relatively identical process to alleviate the effect of fabrication method for better comparison of CW and SN performance on PS reinforcement. Morphology of nanoparticles and their dispersion state in the corresponding nanocomposites were investigated by transmission electron microscopy and field emission scanning electron microscopy, respectively. X-ray diffraction was used for crystallography of nanocomposites and established the transcrystallization only in CW-filled nanocomposites. Nanocomposites comprising quasi-spherical SNs showed higher reinforcement in dynamic mechanical tests compared to the corresponding nanocomposites containing rod-like CWs, which were attributed to more efficient filler/filler and filler/matrix interactions originated from hydrogen bonding in SN-filled nanocomposites.

1. Introduction

Starch is produced by most green plants as an energy store and is the most common carbohydrate in human diets and animal foods (Le Corre, Bras, & Dufresne, 2010). This biopolymer has also found many important industrial applications and accordingly huge amount of production. Bio-based and biodegradable products from starch have raised a tremendous level of attention in the recent years, since sustainable development policies tend to expand with the decreasing reserve of fossil fuel and the growing concern for the environment (Angles & Dufresne, 2001). In the molecular level, starch is a heterogeneous material with two architectures. Amylose is a linear structure of α-1,4 linked glucose units, while amylopectin is a highly branched structure of short α-1,4 chains linked by α-1,6 bonds (Yao, Zhang, & Ding, 2002). Native starch is biosynthesized in the form of semi-crystalline granules made of these two components. Semi-crystalline structure of granules originates from amylopectin chains in double helical configurations (Wang & Copeland, 2013). Starch is not really a thermoplastic but can be converted to a continuous entangled polymeric phase with the aid of water or a nonaqueous plasticizer such as glycerol. Hence, the obtained material can be processed by technologies developed for synthetic polymers (Angellier, Molina-Boisseau, Lebrun, & Dufresne, 2005). In practice, plasticized starch (PS) shows a limited physical performance (Teixeira et al., 2009), so must be reinforced to achieve satisfactory mechanical properties. Various methods that have been used to reinforce PS can be categorized in three main categories: (1) chemical treatment of starch molecule (Avérous, 2004; Cao & Zhang, 2005a, 2005b), (2) mixing PS with other natural or synthetic polymers (Arvanitoyannis, Biliaderis, Ogawa, & Kawasaki, 1998; Avérous, 2004) and (3) using various natural and mineral reinforcers.

Mineral fillers such as talc (Bhatnagar & Hanna, 1996), kaolin (de Carvalho, Curvelo, & Agnelli, 2001) and clay (Wilhelm, Sierakowski, Souza, & Wypych, 2003) and natural reinforcers including plant fibers from different sources (Curvelo, de Carvalho, & Agnelli, 2001), cellulose microfibers (Chen, Cao, Chang, & Huneault, 2008; Dufresne & Vignon, 1998), cellulose whiskers (CWs) (Cao, Chen, Chang, Muir, & Falk, 2008; Teixeira et al., 2009) and starch nanoparticles (SNs) (Angellier, Molina-Boisseau, Dole, & Dufresne, 2006; Viguié, Molina-Boisseau, & Dufresne, 2007) were utilized to reinforce PS up to now. Retaining PS biodegradability and exploiting nanoparticle exclusive properties (such as high modulus and high surface/weight ratio) have increasingly promoted the usage of natural nano-reinforcers in the recent years (Angles & Dufresne, 2001). In addition, chemical similarity of matrix and reinforcer leads to an efficient interface and facilitate stress transfer from matrix to the reinforcer, which improves the final performance of the

* Corresponding author. Tel.: +98 2164542406; fax: +98 21645424.
E-mail addresses: rasool.nasseri@aut.ac.ir (R. Nasseri), mohamadi@aut.ac.ir (N. Mohammadi).

0144-8617/$ – see front matter © 2014 Elsevier Ltd. All rights reserved.
http://dx.doi.org/10.1016/j.carbpol.2014.01.029

composite (Viguié et al., 2007). Therefore, due to the chemical similarity of CWs and SNs with starch based matrix, they have been suggested as promising candidates for PS reinforcement. One of the first studies in PS reinforcement by CWs was reported by Angles and Dufresne (2000, 2001). They showed that due to the accumulation of PS plasticizers on the nanoparticle surfaces, starch molecular movements are facilitated and crystallization of starch chains on the CW surfaces (transcrystallization) occurs. The formation of this soft interphase has been shown to disturb the stress transfer from matrix to fibers and interfere with inter-whisker hydrogen bonding, which leads to decreased final mechanical performance of the nanocomposite (Angles & Dufresne, 2000, 2001). In another study, Teixeira et al. (2009) used cassava bagasse cellulose nanofibrils to reinforce PS and attributed the deficiency of nanoparticles in expected improvement of mechanical properties to transcrystallization. Angellier et al. (2006) studied the reinforcement of waxy maize starch with nanoparticles extracted from the same material. They investigated various factors including glycerol and filler content and aging in different relative humidity on PS mechanical properties. They ascribed the reinforcing effect of nanoparticles to powerful particle/particle and particle/matrix interactions arose from the hydrogen bonding. Viguié et al. (2007) studied the impact of waxy corn SNs on waxy corn PS mechanical properties. They reported 22 times increase in matrix tensile modulus after inclusion of 25 weight percent (wt%) of reinforcer, which was correlated with the powerful interface as a result of hydrogen bondings. García, Ribba, Dufresne, Aranguren, and Goyanes (2009) evaluated the effect of waxy corn SNs in the reinforcement of cassava PS. They related 380% increase of rubbery storage modulus in the presence of 2.5 wt% of SNs to the powerful hydrogen bonding between matrix and particles and among particles themselves. Le Corre et al. (2010), comparing CWs and SNs in PS reinforcement, indicated that the positive impact of SNs in the PS mechanical behavior is more significant than that of CWs. This result is surprising since CWs appear as rod like nanoparticles with the high aspect ratio that should provide a higher reinforcing capability than quasi-spherical starch particles (Angellier et al., 2006). This apparent controversy reveals the need for more precise investigation of the involved factors in reinforcement of PS nanocomposites.

Ishida and Bussi (1991) and recently Li and Yan (2011) have reviewed literatures about transcrystallization in the presence of micro- and nano-scale fibers. They mentioned some factors include similarity in chemical structure and crystalline network of fiber and matrix as the main factors in this phenomenon. Generally, macroscopic properties of starch based nanocomposites are related to reinforcer aspect ratio, fabrication method and filler/filler and filler/matrix interactions (Samir, Alloin, & Dufresne, 2005). Accordingly, similar fabrication procedure can help the precise evaluation of two other remaining factors.

Owing to structural similarity with the matrix, cellulose whiskers and starch nanoparticles have been chosen for PS reinforcement in the current research. CWs and SNs were extracted through acid hydrolysis using sulfuric acid to fulfill the similar surface groups and interactions among nanoparticles and also with the matrix. CW-filled and SN-filled nanocomposites were then prepared with relatively identical process in order to alleviate the effect of fabrication method for better evaluation of CWs and SNs performance and the involving surface phenomena on PS reinforcement. After morphological investigation and crystallography of nanocomposites, their reinforcement efficiency were investigated by dynamic mechanical thermal analysis (DMTA), and then efficiency of nanoparticles on PS reinforcement was scrutinized based on particle/particle and particle/matrix interactions and surface phenomena.

2. Materials and methods

2.1. Materials

Food-grade wheat starch (from Kerman, Iran) containing about 27% amylose and hygiene cotton fibers were used in this study. Glycerol (98%) and sulfuric acid (98%) were supplied by Dr. Mojallali Chemical Company.

2.2. Cellulose whisker extraction

CWs were extracted from cotton fibers by Roohani et al. (2008) method. Firstly, 5 g cotton fibers were finely chopped. Chopped fibers were then added to 64 wt% sulfuric acid aqueous solution (fibers per solution ratio 1/20). Acid hydrolysis of cotton fibers were carried out at 45 °C under vigorous mechanical stirring (700 rpm) for 45 min. Then, the ensuing suspension was diluted with cold distilled water and neutralized by centrifugation and dialysis against distilled water. After dialysis, the suspension pH reached 6–7. In order to achieve individual particles, the resulting suspension was submitted to an ultrasonic treatment for 10 min in an ice bath. For the direct use in the nanocomposite preparation, resulting suspension was concentrated to more than 5 wt% in a moderate temperature under slow stirring and was stored in the refrigerator. The concentration of suspension was precisely measured by completely drying a certain amount of it (5 g) and calculating the weight difference before and after drying.

2.3. Starch nanoparticle extraction

SNs were extracted from wheat starch based on Angellier, Choisnard, Molina-Boisseau, Ozil, and Dufresne (2004) method. Briefly described, 36.725 g starch was mixed with 250 ml of 3.16 M aqueous solution of sulfuric acid and stirred vigorously (400 rpm) for 5 days at 40 °C. The resultant suspension was then diluted with cold distilled water and neutralized by centrifugation and dialysis against distilled water. After dialysis, the suspension pH reached 5–7. In order to achieve individual particles, the resulting suspension was submitted to an ultrasonic treatment for 5 min in an ice bath. For the direct use in the nanocomposite preparation, resultant suspension was concentrated to more than 5 wt% in a moderate temperature under slow stirring and was stored in the refrigerator. The concentration of suspension was precisely measured by completely drying a certain amount of it (5 g) and calculating the weight difference before and after drying.

2.4. Starch matrix preparation

To prepare the matrix, 3 g starch was first dispersed in the mixture of 1.5 g glycerol and 25.5 g distilled water. The gelatinization was performed in a 100 m two-necked glass reactor under vigorous stirring (200 rpm) at 120 °C for 30 min. After mixing, the resulting suspension was casted in a glass Petri dish and dried in a vacuum oven at 50 °C for 24 h.

2.5. Nanocomposite preparation method

PS nanocomposites containing 10, 15 and 20 wt% of nanoparticles based on the total weight of starch and glycerol (Nanoparticle/starch + glycerol) were prepared according to the following procedures.

2.5.1. Cellulose whisker-filled nanocomposites

Cellulose whisker suspension containing predetermined amount of particles was diluted until its water content reached 25.5 g. To ensure the homogeneity, suspension was submitted to

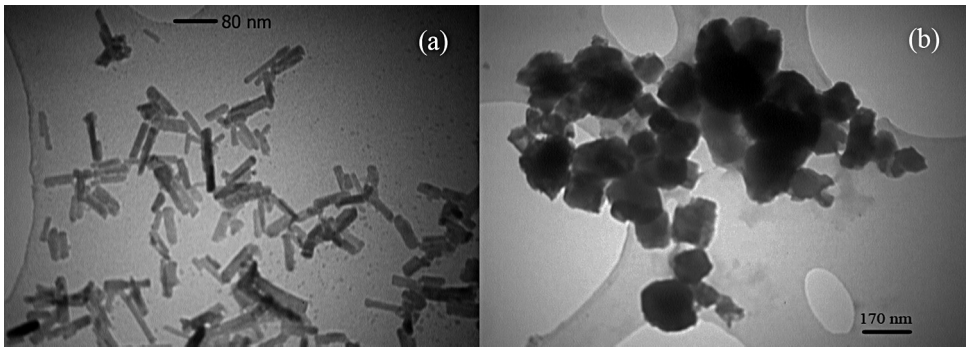

Fig. 1. Transmission electron micrograph of (a) CWs and (b) SNs.

an ultrasonic treatment for 2 min in an ice bath. Then, 3 g starch was mixed with 1.5 g glycerol and the homogenized whisker suspension. In all samples the starch, glycerol and water contents were fixed at 3 g, 1.5 g and 25.5 g, respectively. The resulting paste was then transferred to 100 ml two-necked glass reactor and vigorously stirred (200 rpm) for 30 min in 120 °C oil bath. Afterward, the suspension was casted in a glass Petri dish and dried in a vacuum oven at 50 °C for 24 h.

2.5.2. Starch nanoparticle-filled nanocomposites

The preparation of SN-filled nanocomposite must be carried out in two steps in order to inhibit the gelatinization of starch nanoparticles. At the first step, 3 g starch was dispersed in the mixture of 1.5 g glycerol and 25.5 g distilled water. The obtained paste was then transferred to a 100 ml two-necked glass reactor and vigorously stirred (200 rpm) for 20 min in 120 °C oil bath. Complete gelatinization of starch was confirmed by the disappearance of ghosts within the starch gel using optical microscopy, Fig. A1 of supplementary data. Subsequently, the oil bath was cooled to 40 °C (under the gelatinization temperature of starch) and the suspension of starch nanoparticles was added in the appropriate amount without further dilution to prevent plenty amount of excess water and prolongation of the drying step. In all samples the starch and glycerol contents were fixed at 3 g and 1.5 g, respectively. The mixture was then stirred for 10 min before casting in a glass Petri dish and dried in vacuum oven at 50 °C for 24 h.

2.6. Transmission electron microscopy (TEM)

Transmission electron microscopy was performed to confirm nanoparticle extraction and to investigate their morphology. In this regards, a droplet of nanoparticle suspensions (0.3 wt% for CW and 0.05 wt% for SN) was deposited on a carbon coated steel grid. TEM images were obtained by a Philips CM 120 transmission electron microscope with an acceleration voltage of 120 kV. CellProfiler image analyzing software was used to measure the particle size.

2.7. Field emission scanning electron microscopy (FESEM)

To investigate the morphology of the nanocomposites, field emission scanning electron microscopy was performed on nanocomposites with a Hitachi S4160 instrument using 5 kV secondary electrons. The specimens were frozen under liquid nitrogen, then fractured, mounted, coated with gold and observed.

2.8. Wide angle X-ray diffraction (WAXRD)

The X-ray diffraction patterns were studied for crystallography of nanocomposite using a diffractometer with CuKα_1 X-ray source and wavelength of 1.5406 Å operating at 40 kV and 30 mA radiation (Inel EQUINOX 3000). Scattered filament current was detected in the range of $2\theta = 5–40°$, at a speed of 2°/min.

2.9. Dynamic mechanical thermal analysis (DMTA)

Dynamic mechanical measurements were performed in order to characterize the thermomechanical behavior of these systems. DMTA tests were carried out with a Netzsch 242C DMTA instrument, using a single cantilever bending method. The dynamic storage modulus (E') and damping factor ($\tan\delta$) were measured as a function of temperature from −120 °C to 140 °C, at a constant heating rate of 5 °C/min and a frequency of 1 Hz.

3. Results and discussion

3.1. Morphological characterization of nanoparticles and nanocomposites

Transmission electron micrographs of CWs are presented in Fig. 1a. The suspension was constituted of individual cellulose whiskers with length (L) of 87 ± 28 nm, and diameter (d) of 15 ± 3 nm. The average aspect ratio (L/d) of whiskers is therefore obtained as 6 ± 2.

Scanning electron micrographs of CW-filled nanocomposites are shown in Fig. 2. In the nanocomposite images the presence of whiskers in the form of shiny white dots is obvious. These shiny dots are cross section of CWs and show an appropriate dispersion of nanoparticles in the matrix. Their measured diameters were around 70 nm that was much higher than real diameter of whiskers. Due to the negative surface charges of CWs and their rigid high crystalline nature, the aggregation cannot occur among them even within the collisions during the nanocomposite preparation. The negative surface charges originated from SO_3^- generation during the sulfuric acid hydrolysis. Various factors such as non-circular cross section of fibers or charge concentration effect (Angles & Dufresne, 2000) due to emergence of whiskers from the observed surface may cause such a controversy.

Transmission electron micrograph of starch nanoparticles is displayed in Fig. 1b. Quasi-spherical SNs have an average size around 100 nm and form aggregates of 1–3 μm, showing very close resemblance to the morphological characteristics previously reported for wheat starch nanoparticles (Le Corre, Bras, & Dufresne, 2011). The uneven surface of nanoparticles may be because of the defects in their crystalline structure.

In scanning electron micrographs of SN-filled nanocomposite, nanoparticles are observed as white dots (Fig. 3). These images show relatively appropriate dispersion of nanoparticles in the matrix. The particle diameter was measured around 200–700 nm, which is much higher than single particle diameter. Agglomeration of few particles (2–4) and charge concentration effect due to

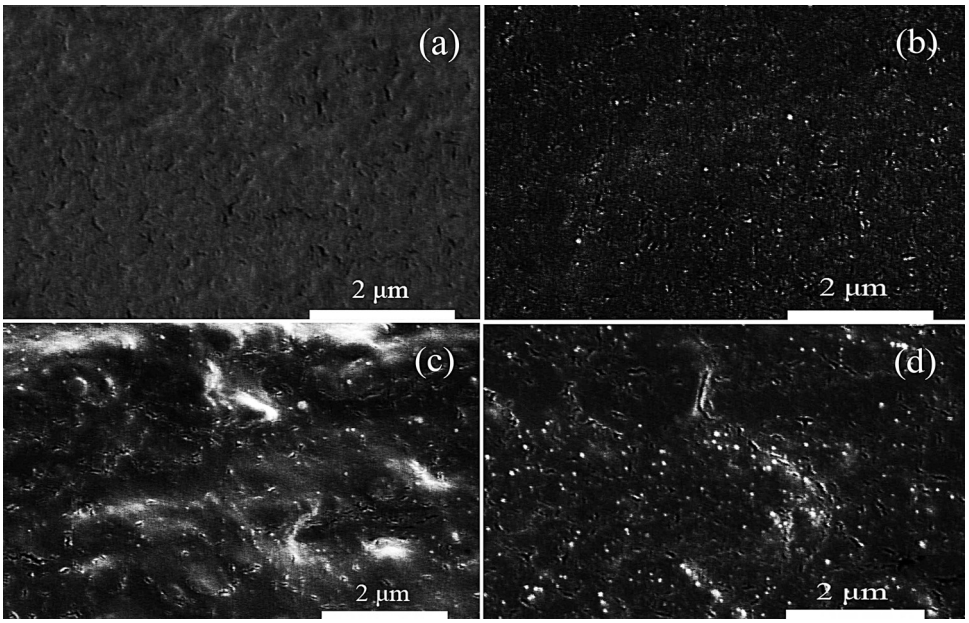

Fig. 2. Scanning electron micrographs of CW-filled nanocomposites containing (a) 0 wt%, (b) 10 wt%, (c) 15 wt% and (d) 20 wt% CWs.

the emergence of particles from the observed surface may have this consequence. Unlike CWs, SNs are not rigid particles due to the low crystallinity and can partially merge into each other during collision in a high temperature process.

3.2. Wide angle X-ray diffraction (WAXRD)

Diffractogram of neat PS is presented in Fig. 4a. Peaks in 2θ 5.51°, 17.2° and 22.3° are characteristics of B type starch crystals (Angles & Dufresne, 2000; Cao et al., 2008) and a tiny peak in range of 18°–19.5° is ascribed to V_h type starch crystals originated from the amylose-lipid complex (Buléon, Colonna, Planchot, & Ball, 1998).

Diffractograms of CW-filled nanocomposites, neat matrix and CW are shown in Fig. 4b. Peaks in 2θ 15°, 16.5° and 22.8° in CW diffractogram establish the I cellulose structure (Lewin & Roldan, 1975). Diffractograms of nanocomposites comprising SNs, neat matrix and SN are also presented in Fig. 4c. Displaying the diffraction pattern of both A type starch crystals with strong reflections at 2θ 15.1°, 17.2°, 18.1° and 23.2° and B type starch crystals in SN diffractogram establish the coincidence of both A- and B-type or C-type crystal pattern.

In Fig. 4b, increase in peak amplitudes is noticeable in the range of CW diffraction peaks in nanocomposite diffractograms. Such observation is expected due to the increase in whisker content in the matrix, but since no peak is distinguished in diffraction pattern of the matrix and particles in $2\theta = 25.5°$ the presence of a peak in this 2θ must be attributed to the transcrystallization of starch chains on the CW surfaces (Angles & Dufresne, 2000; Teixeira et al., 2009). During the extraction process, the nanoparticle surfaces become negatively charged as a result of hydroxyl group esterification of cellulose or starch molecules by sulfate ions. Consequently, PS plasticizers (glycerol and water) present more affinity to the

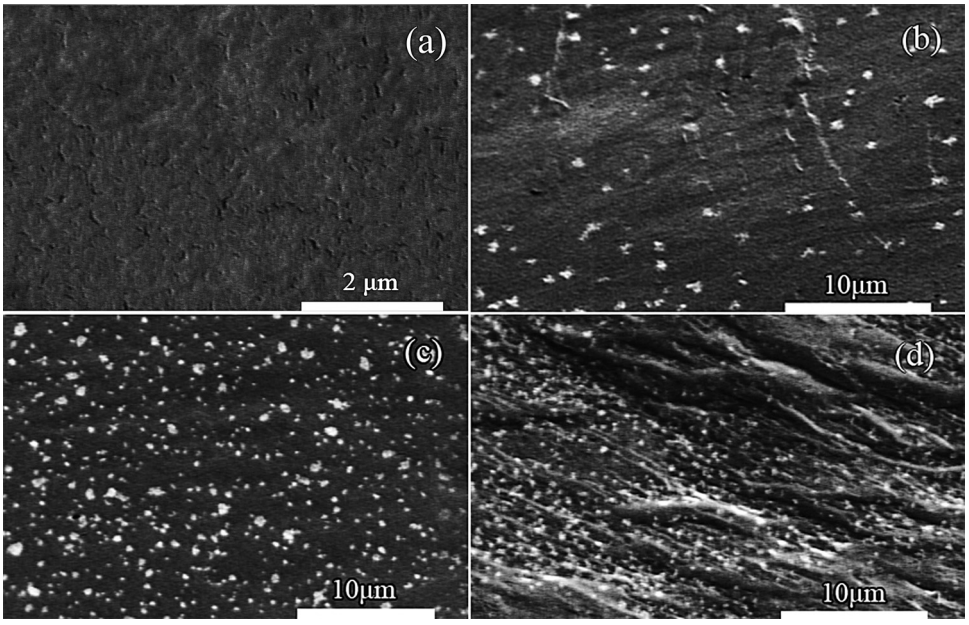

Fig. 3. Scanning electron micrographs of SN-filled nanocomposites containing (a) 0 wt%, (b) 10 wt%, (c) 15 wt% and (d) 20 wt% SNs.

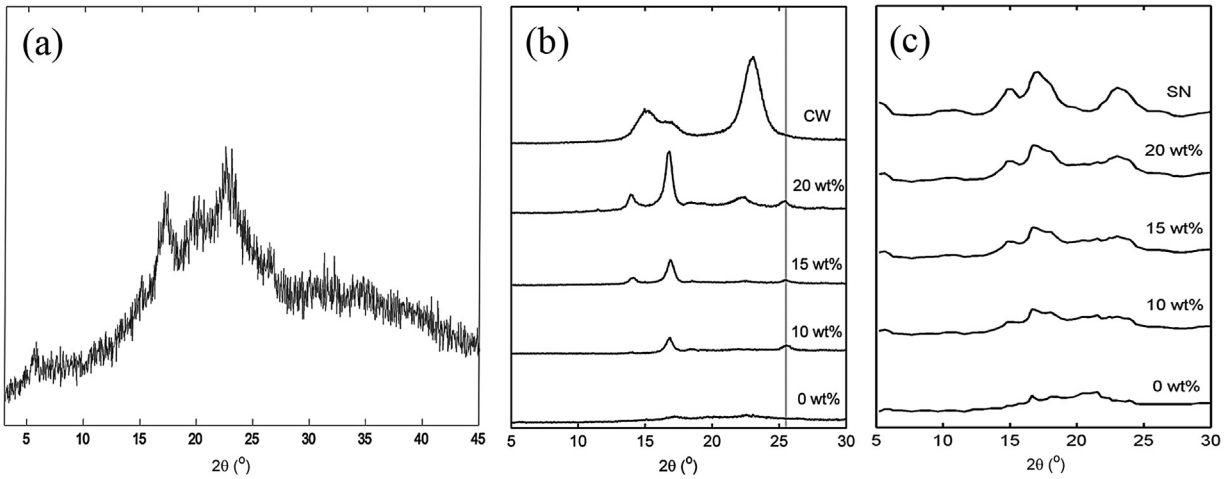

Fig. 4. Diffractograms of (a) neat PS, (b) CW-filled nanocomposites, neat matrix and CW and (c) SN-filled nanocomposites, neat matrix and SN. Vertical axis of (a), (b) and (c) parts of this figure has different scales.

CW surfaces than nanocomposite matrix (Angles & Dufresne, 2000; Teixeira et al., 2009), so they migrate, accumulate and facilitate the chain movements in the interface regions. Additionally, near-perfect crystalline structure of CWs provides an efficient nucleating agent for transcrystallization (Angles & Dufresne, 2000). Such as the neat matrix, a tiny peak in range of 2θ 18°–19.5° in nanocomposite diffractograms can be ascribed to V_h type starch crystals originated from the amylose-lipid complexes. Orientated crystallization of amylose from a solution on cellulose was previously reported in the literature (Helbert & Chanzy, 1994). In SN-filled nanocomposites, amplification of peaks in the range of SN diffraction peaks is also obvious with the increase in nanoparticle content. Nonetheless, no additional peak emerges in diffraction patterns of nanocomposites (Fig. 3c). Consequently, it can be concluded that transcrystallization does not occur in SN-filled nanocomposites. In the case of SN-filled nanocomposites the migration of main plasticizers toward the filler/matrix interface is also expectable due to the negative surface charges, but the migrated plasticizers can be absorbed into amorphous regions of nanoparticles. Accordingly, the regional plasticization of starch chain in vicinity of SNs cannot occur. In addition, the uneven surface and defects in crystalline structure of SNs may disturb their role as the crystal nuclei.

3.3. Dynamic mechanical behavior

DMTA results showed the success in PS reinforcement with CWs and SNs (cf. Figs. 5a and 6a). Fig. 5a presents the storage modulus of CW-filled nanocomposite as a function of temperature. As shown, two decaying steps in curves establish the presence of two distinguishable phases in the nanocomposites. For the films that contained CWs, the magnitude of two-step modulus drop is strongly reduced. Starting points of the curves were transferred to 1 GPa. This is justified by the fact that in this temperature range the difference between the elastic modulus of the cellulose whiskers and that of the starch matrix was not high enough to easily appreciate reinforcing effect. Besides, it can minimize the errors of dimension measurements of the specimens (Angles & Dufresne, 2001; Viguié et al., 2007).

For investigation of biphasic behavior and glass transitions of systems, damping factor ($\tan\delta$) against temperature curves of CW-filled nanocomposites are presented in Fig. 5b. These curves obviously confirm the biphasic nature of the nanocomposites. The partial phase separation of glycerol and starch during the film drying makes two phases. Although, lower T_g was attributed to the glycerol-rich phase, the starch-rich phase has higher glass transition temperature (Angles & Dufresne, 2000).

When the filler content increases, the temperature position of the low-temperature transition (α_1), remains roughly constant whereas the increase in temperature position of high-temperature transition (α_2), is pronounced. The apparent unalteration of the T_g evolution of the glycerol-rich fraction in the presence of CWs results most probably from the fact that these domains occur as inclusions in the continuous phase constituted of starch-rich domains. Therefore, the CWs are most probably in direct contact with starch-rich domains rather than glycerol-rich domains when dispersed in the plasticized starch matrix (Angles & Dufresne, 2000), Fig. A2 of supplementary data. The increase in temperature position of α_2 relaxation in 10 and 15 wt% CW-filled nanocomposites was relatively low (4.5 °C and 8.5 °C, respectively) but in the case of 20 wt% filled sample was quite significant and about 43.5 °C (Table 1). Three phenomena could explain the increase of T_g in starch-rich domains in the presence of CWs. The first one is the likely strong affinity of starch molecules with the reactive cellulose surface due to the high density of hydroxyl groups in both of them. This coupling effect could result in a restricted molecular mobility of starch molecules in contact with the whisker surfaces that could be strong enough to affect the global flexibility of the starch matrix. The second explanation could be the partial migration of glycerol toward the filler/matrix interface due to the higher affinity for the CW surface than for the starch-based matrix. A migration of the main plasticizer from the starch-rich domains could result, decreasing the plasticizing efficiency of the glycerol for the starch matrix. This phenomenon should result in an increase of T_g. Another explanation could be the transcrystallization phenomenon that could result in a restricted mobility of amorphous starch chains in the vicinity of the crystallite-coated filler surface, because crystalline domains of

Table 1
Glass transition temperatures associated with the transitions of glycerol-rich ($T_{g,1}$) and starch-rich ($T_{g,2}$) domains of nanocomposites.

Filler	wt (%)	$T_{g,1}$ (°C)	$T_{g,2}$ (°C)
CW	0	−37.5	43.5
	10	−45	48
	15	−38.5	52
	20	−36.5	87
SN	0	−37.5	43.5
	10	−36.5	15
	15	−38	59
	20	−37.5	62

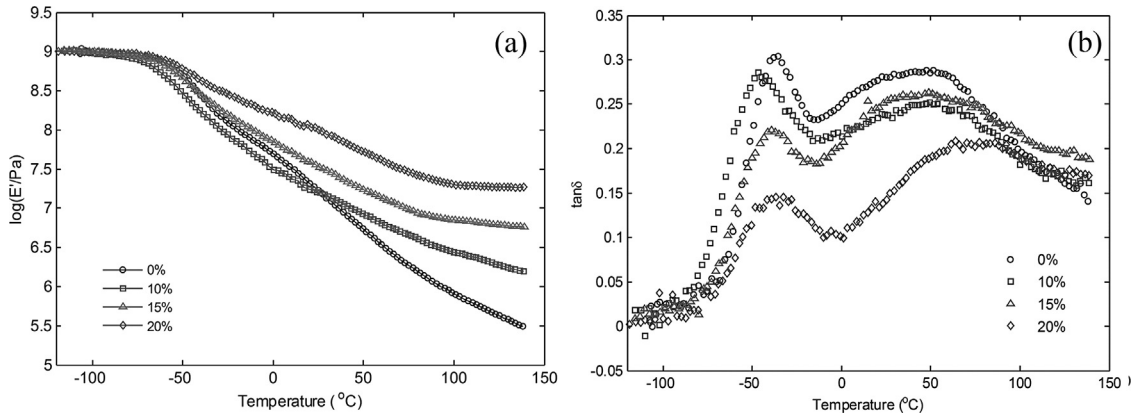

Fig. 5. (a) Storage modulus and (b) damping factor of CW-filled nanocomposite as a function of temperature.

starch act as physical cross-links (Angles & Dufresne, 2000). Accordingly, it is expected that with an increase in CW content and active surfaces in the matrix, α_2 transition shifts to higher temperatures (Angles & Dufresne, 2001). The relatively great shift in temperature position of α_2 in 20 wt% filled case could have one another reason. In this highly filled sample CWs can make a percolated network in the matrix (percolation threshold of CWs with aspect ratio 6 is about 16 wt%; Samir et al., 2005). Migration of plasticizer toward the filler/PS interface, however, leading to the formation of a soft interphase around the fillers and interfere with development of a powerful percolated network but this loose network can partially restrict mobility of starch chains (Fig. A2 of supplementary data). This further restriction can cause the substantial shift in temperature position of α_2 in the most concentrated case. The magnitude of both relaxations decreases as the whiskers content increases. This phenomenon is ascribed to both the decrease of the relaxing entities participating in the relaxation process and to the concomitant lowering of the modulus drop up on whiskers addition (Angles & Dufresne, 2001) (Fig. 5b). The percolated network in the most concentrated case leading to the substantial lowering of second modulus drop also caused the more pronounced magnitude decrease of α_2 relaxation. The α_2 relaxation peaks were broader than those of α_1 relaxation. This dynamic heterogeneity occurs due to the different behaviors of main relaxation of linear or branched starch chains with various lengths which are partially involved in crystals or hydrogen interactions with CW surfaces. But in the case of glycerol-rich phase lack of theses interactions leads to a more uniform dynamic behavior and a narrow damping peak.

The effect of SNs on PS reinforcement is also obvious (Fig. 6a). For the films comprising SNs, the magnitude of the two-step modulus drop is significantly reduced. The starting points of the curves were transferred to 1 GPa. This is also justified by the fact that the reinforcing effect of SNs in this temperature range should be low. Besides, it can minimize the errors of dimension measurements of the soft specimens (Angles & Dufresne, 2001; Viguié et al., 2007). Two decaying steps in storage modulus of SN-filled nanocomposites reveal the biphasic nature of these systems.

Damping factor of SN-filled nanocomposites also confirms the partial phase separation of starch and glycerol leading to coexistence of two phases (Fig. 6b). It is observed that the T_g associated with the glass transition of glycerol-rich domains ($T_{g.1}$) remains roughly constant regardless the SNs content. It can be concluded that the fillers are not in direct contact with the glycerol-rich domains. On the contrary, when the SN content increases the T_g associated with the glass transition of starch-rich domains ($T_{g.2}$) is found to decrease at first and then increase (Table 1). The initial decrease of $T_{g.2}$ in presence of 10 wt% SNs could be explained with the plasticization effect of filler under percolation threshold (percolation threshold of SNs is about 10 wt%; Angellier et al., 2006) leading to enhanced mobility of starch chain (Liu, Zhong, Chang, Li, & Wu, 2010). The average radius of gyration of wheat starch molecules is about 170 nm (Aberle & Burchard, 1997) which is bigger than the average size of SNs (~100 nm). Consequently, the starch particles can increase the interchain distances and facilitate molecular motions, but CWs with the diameter around 15 nm cannot cause this effect. The increase of $T_{g.2}$ in higher SN contents is an indication that the percolated network of fillers can hinder the molecular mobility of starch chains. It is most probably ascribed to a direct contact between the starch-rich domains of the matrix and SNs, and to strong filler/filler and filler/matrix

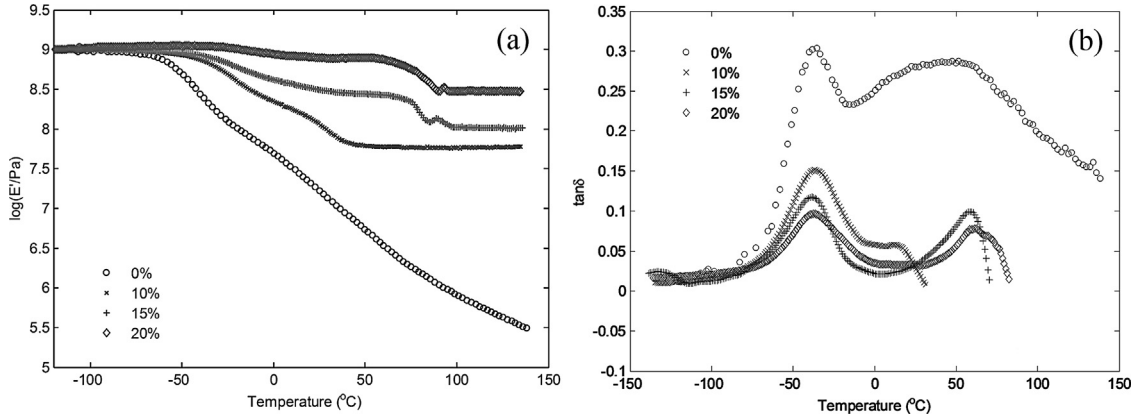

Fig. 6. (a) Storage modulus and (b) damping factor of SN-filled nanocomposite as a function of temperature.

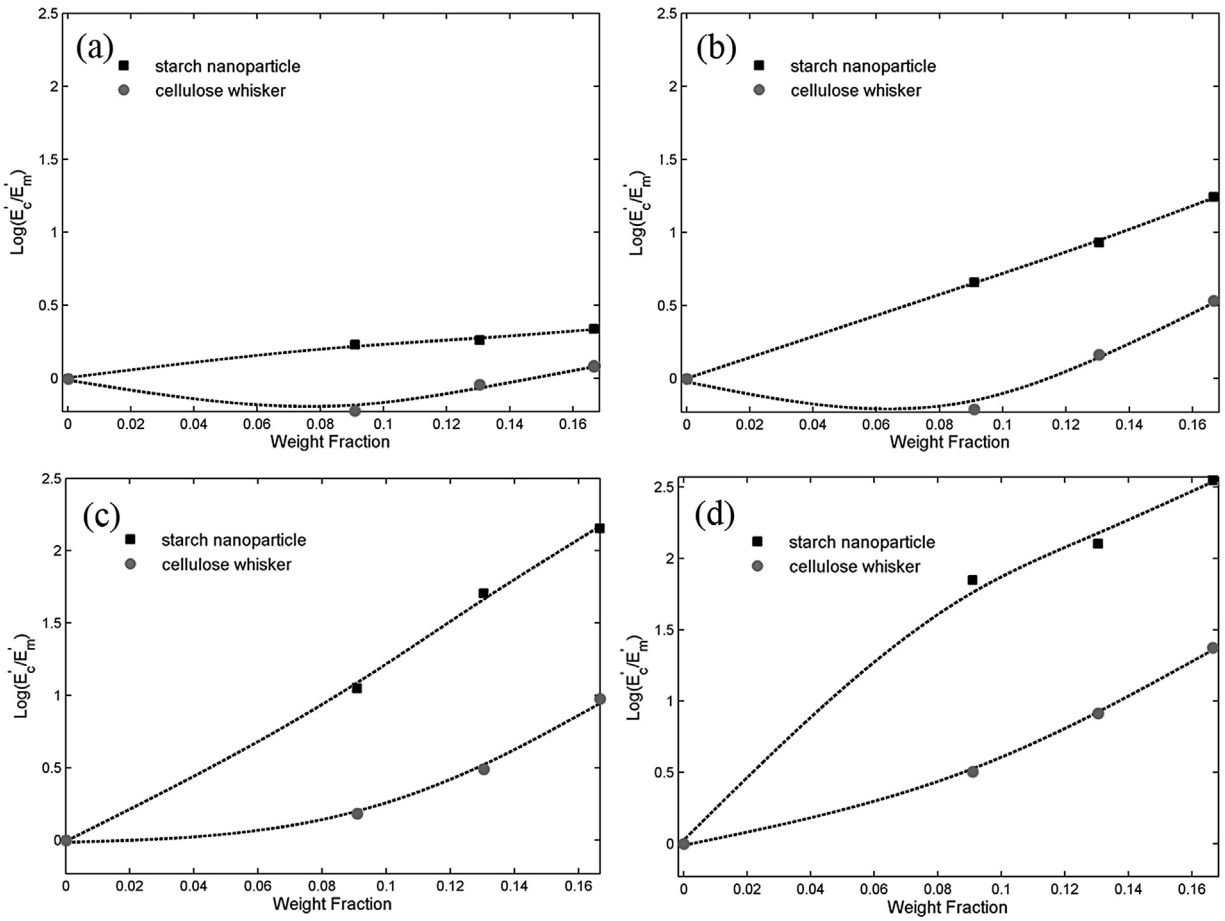

Fig. 7. Performance comparison of CWs and SNs in PS reinforcement in various temperatures (a) −50 °C, (b) 0 °C. (c) 50 °C and (d) 100 °C. Weight fractions were calculated assuming complete removal of water.

interactions due to the hydrogen bondings (Angellier et al., 2006). It is expected that the glycerol partially migrate into the surface of starch nanoparticles and absorb in their amorphous regions. A migration of the main plasticizer from the starch-rich domains could result, decreasing the plasticizing efficiency of the glycerol for the starch matrix. It could be another explanation for the increase of starch-rich phase glass transition. Decrease in the magnitude of both relaxations up on SNs addition was considerable and was mainly due to the magnitude diminution of the two-step modulus drop (Fig. 6a) and decrease of the proportions of both glycerol and starch as the participants to the relaxations (Fig. 6b) (Viguié et al., 2007). The concomitant lowering of the modulus drops up on SNs addition is more conspicuous. Consequently, the magnitude diminution of both relaxations was more considerable in SN-filled nanocomposites. The high-temperature relaxation peaks in these nanocomposites are narrower than those of CW-filled nanocomposites (Fig. 5b and 6b). Efficient filler/matrix interactions (in absence of migrated glycerol layer) due to the powerful hydrogen bonding in SN-filled nanocomposites interfere with main relaxation of starch molecules in starch-rich phase and make the more uniform material dynamic behavior which leads to narrower damping peak.

For better efficiency comparison of CWs and SNs in the PS reinforcement, the evolution of logarithm of normalized storage modulus was evaluated in four temperatures (Fig. 7). In this regard, the experimental values of matrix and nanocomposites storage modulus (E'_C and E'_m) were considered.

This result is surprising since CWs appear as rod like nanoparticles with a restively high aspect ratio that should result in a higher reinforcing capability than quasi-spherical starch nanoparticles (Angellier et al., 2006). On the other hand, even in the highest CW concentration in which loose percolated network may form; CW-filled nanocomposites do not present a high mechanical performance. With the increase in temperature up to low- and high-temperature transitions of nanocomposites the reinforcement efficiency of both nanoparticles increases but for SNs it is more pronounced (Fig. 7a–d). The deficiency of CWs in PS reinforcement may be due to migration of glycerol toward the filler/matrix interface leading to the formation of a soft interphase around the fillers which interfere with development of a powerful percolated network. As a result, the main effect of rod like particles is practically omitted. Besides, this migration facilitates the crystallization of starch chains on CW surfaces. Transcrystals cannot preserve high amount of plasticizer, so glycerol leaks throughout the chains during the crystallization and add to the glycerol-rich layer in the vicinity of whiskers. The presence of this layer immediately after the rigid rod like CWs can absolutely disturb the stress transfer from matrix to fillers (Fig. A2 of supplementary data). On the other hand, SNs can absorb the migrated glycerol into their amorphous regions. Furthermore, uneven surface and defects in crystalline structure of SNs interfere with nucleation role of these nanoparticles and prevent the transcrystallization (Fig. A2 of supplementary data). Therefore they can form a stiff percolated network due to powerful hydrogen bonding leading to the higher performance

in PS reinforcement. The schematic drawing of nanocomposite microstructures are presented in Fig. A2 of supplementary data.

4. Conclusions

In this study cellulose whiskers and starch nanoparticles were extracted trough acid hydrolysis using sulfuric acid to fulfill the similar surface groups and interactions among nanoparticles and also with the matrix. CW-filled and SN-filled nanocomposites were then prepared with relatively identical process in order to alleviate the effect of fabrication method for better comparison of CWs and SNs performance on the PS reinforcement. Crystallography of nanocomposites, however, showed the presence of a new diffraction peak in $2\theta = 25.5^{\circ}$ in CW-filled nanocomposites, confirmed no new diffraction peak in SN-filled nanocomposites. This new diffraction peak in CW-filled nanocomposites was attributed to transcrystallization of starch chains on whisker surfaces. The comparison of dynamic mechanical behavior of nanocomposites containing these two nanoparticles showed noticeable differences. Since the matrixes of nanocomposites were the same, these differences were ascribed to various filler/filler and filler/matrix interactions and different surface phenomena. Accumulation of migrated plasticizers toward the interface and transcrystallization in CW-filled nanocomposites disturb the stress transfer from matrix to fillers and prevent the percolation of fillers in the matrix. On the other hand, hydrogen bondings in the absence of plasticizer layer and transcrystals cause more efficient filler/filler and filler/matrix interactions in case of SN-filled nanocomposite. In addition, in these nanocomposites percolation of nanoparticles could happen. These differences surprisingly make SNs more efficient in PS reinforcement than CWs.

Acknowledgments

The authors gratefully acknowledge Dr. Mehdi Roohani (Mohaghegh Ardabili University) for worthwhile guides in cellulose whisker extraction procedure and Dr. Erfan Dashtimoghadam for valuable discussions.

Appendix A. Supplementary data

Supplementary material related to this article can be found, in the online version, at http://dx.doi.org/10.1016/j.carbpol.2014.01.029.

References

Aberle, T., & Burchard, W. (1997). Starches in semidilute aqueous solution. *Starch – Stärke*, *49*, 215–224.
Angellier, H., Molina-Boisseau, S., Lebrun, L., & Dufresne, A. (2005). Processing and structural properties of waxy maize starch nanocrystals reinforced natural rubber. *Macromolecules*, *38*, 3783–3792.
Angellier, H., Molina-Boisseau, S., Dole, P., & Dufresne, A. (2006). Thermoplastic starch-waxy maize starch nanocrystals nanocomposites. *Biomacromolecules*, *7*, 531–539.
Angellier, H., Choisnard, L., Molina-Boisseau, S., Ozil, P., & Dufresne, A. (2004). Optimization of the preparation of aqueous suspensions of waxy maize starch nanocrystals using a response surface methodology. *Biomacromolecules*, *5*, 1545–1551.
Angles, M. N., & Dufresne, A. (2000). Plasticized starch/tunicin whiskers nanocomposites. 1. Structural analysis. *Macromolecules*, *33*, 8344–8353.
Angles, M. N., & Dufresne, A. (2001). Plasticized starch/tunicin whiskers nanocomposite materials. 2. Mechanical behavior. *Macromolecules*, *34*, 2921–2931.
Arvanitoyannis, I., Biliaderis, C. G., Ogawa, H., & Kawasaki, N. (1998). Biodegradable films made from low-density polyethylene (LDPE), rice starch and potato starch for food packaging applications: Part 1. *Carbohydrate Polymers*, *36*, 89–104.
Avérous, L. (2004). Biodegradable multiphase systems based on plasticized starch: A review. *Journal of Macromolecular Science, Part C: Polymer Reviews*, *44*, 231–274.
Bhatnagar, S., & Hanna, M. A. (1996). Effect of talc on properties of corn starch extrudates. *Starch – Stärke*, *48*, 94–101.
Buléon, A., Colonna, P., Planchot, V., & Ball, S. (1998). Starch granules: Structure and biosynthesis. *International Journal of Biological Macromolecules*, *23*, 85–112.
Cao, X., & Zhang, L. (2005a). Miscibility and properties of polyurethane/benzyl starch semi-interpenetrating polymer networks. *Journal of Polymer Science Part B: Polymer Physics*, *43*, 603–615.
Cao, X., & Zhang, L. (2005b). Effects of molecular weight on the miscibility and properties of polyurethane/benzyl starch semi-interpenetrating polymer networks. *Biomacromolecules*, *6*, 671–677.
Cao, X., Chen, Y., Chang, P., Muir, A., & Falk, G. (2008). Starch-based nanocomposites reinforced with flax cellulose nanocrystals. *Express Polymer Letters*, *2*, 502–510.
Chen, Y., Cao, X., Chang, P. R., & Huneault, M. A. (2008). Comparative study on the films of poly (vinyl alcohol)/pea starch nanocrystals and poly (vinyl alcohol)/native pea starch. *Carbohydrate Polymers*, *73*, 8–17.
Curvelo, A. A. S., de Carvalho, A. J. F., & Agnelli, J. A. M. (2001). Thermoplastic starch–cellulosic fibers composites: Preliminary results. *Carbohydrate Polymers*, *45*, 183–188.
de Carvalho, A. J. F., Curvelo, A. A. S., & Agnelli, J. A. M. (2001). A first insight on composites of thermoplastic starch and kaolin. *Carbohydrate Polymers*, *45*, 189–194.
Dufresne, A., & Vignon, M. R. (1998). Improvement of starch film performances using cellulose microfibrils. *Macromolecules*, *31*, 2693–2696.
García, N. L., Ribba, L., Dufresne, A., Aranguren, M. I., & Goyanes, S. (2009). Physicomechanical properties of biodegradable starch nanocomposites. *Macromolecular Materials and Engineering*, *294*, 169–177.
Helbert, W., & Chanzy, H. (1994). Oriented growth of V amylose n-butanol crystals on cellulose. *Carbohydrate Polymers*, *24*, 119–122.
Ishida, H., & Bussi, P. (1991). Surface induced crystallization in ultrahigh-modulus polyethylene fiber-reinforced polyethylene composites. *Macromolecules*, *24*, 3569–3577.
Le Corre, D., Bras, J., & Dufresne, A. (2010). Starch nanoparticles: A review. *Biomacromolecules*, *11*, 1139–1153.
Le Corre, D., Bras, J., & Dufresne, A. (2011). Influence of botanic origin and amylose content on the morphology of starch nanocrystals. *Journal of Nanoparticle Research*, *13*, 7193–7208.
Lewin, M., & Roldan, L. G. (1975). The oxidation and alkaline degradation of Mercerized cotton: A morphological study. *Textile Research Journal*, *45*, 308–314.
Li, H., & Yan, S. (2011). Surface-induced polymer crystallization and the resultant structures and morphologies. *Macromolecules*, *44*(3), 417–428.
Liu, D., Zhong, T., Chang, P. R., Li, K., & Wu, Q. (2010). Starch composites reinforced by bamboo cellulosic crystals. *Bioresource Technology*, *101*, 2529–2536.
Roohani, M., Habibi, Y., Belgacem, N. M., Ebrahim, G., Karimi, A. N., & Dufresne, A. (2008). Cellulose whiskers reinforced polyvinyl alcohol copolymers nanocomposites. *European Polymer Journal*, *44*, 2489–2498.
Samir, M. A. S. A., Alloin, F., & Dufresne, A. (2005). Review of recent research into cellulosic whiskers, their properties and their application in nanocomposite field. *Biomacromolecules*, *6*, 612–626.
Teixeira, E. d. M., Pasquini, D., Curvelo, A. A. S., Corradini, E., Belgacem, M. N., & Dufresne, A. (2009). Cassava bagasse cellulose nanofibrils reinforced thermoplastic cassava starch. *Carbohydrate Polymers*, *78*, 422–431.
Viguié, J., Molina-Boisseau, S., & Dufresne, A. (2007). Processing and characterization of waxy maize starch films plasticized by sorbitol and reinforced with starch nanocrystals. *Macromolecular Bioscience*, *7*, 1206–1216.
Wang, S., & Copeland, L. (2013). Molecular disassembly of starch granules during gelatinization and its effect on starch digestibility: A review. *Food & Function*, *4*, 1564–1580.
Wilhelm, H. M., Sierakowski, M. R., Souza, G. P., & Wypych, F. (2003). Starch films reinforced with mineral clay. *Carbohydrate Polymers*, *52*, 101–110.
Yao, Y., Zhang, J., & Ding, X. (2002). Structure–retrogradation relationship of rice starch in purified starches and cooked rice grains: A statistical investigation. *Journal of agricultural and food chemistry*, *50*, 7420–7425.